Accepted Manuscript

Submission Date: 2023-10-23
Accepted Date: 2024-08-17
Accepted Manuscript online: 2024-10-04

Thrombosis and Haemostasis

Cardiac repair after myocardial infarction is controlled by a complement C5a receptor 1-driven signaling cascade

Yaw Asare, Sakine Simsekyilmaz, Janine Köhncke, Gansuvd Shagdarsuren, Mareike Staudt, Heidi Noels, Andreas Klos, Johannes Fischer, Jürgen Bernhagen, Alma Zernecke, Elisa A. Liehn, Erdenechimeg Shagdarsuren.

Affiliations below.

DOI: 10.1055/a-2434-4905

Please cite this article as: Asare Y, Simsekyilmaz S, Köhncke J et al. Cardiac repair after myocardial infarction is controlled by a complement C5a receptor 1-driven signaling cascade. Thromb Haemost 2024. doi: 10.1055/a-2434-4905

Conflict of Interest: The authors declare that they have no conflict of interest.

This study was supported by German Center for Cardiovascular Research, DZHK B 20-004 Extern/81X2600258 to J. B, Deutsche Forschungsgemeinschaft (http://dx.doi.org/10.13039/501100001659), (CRC 1123 [A3] to JB,(DFG; CRC 1123 [B3]; and AS 575/1-1) grant to Y. A,DFG (GU1223/3-1) to ES

Abstract:
Cardiac repair following myocardial infarction is important in regenerating functionally viable myocardium to prevent cardiac death. Previous studies have linked C5aR1 to cardiac regeneration and inflammation. However, C5a receptor-driven responses during the late phases, up to 4 weeks of the infarction insult – a time window that specifically reflects the outcome of the repair process – and the underlying mechanisms are poorly defined. Here, we show that C5ar1, but not C5ar2, deficiency attenuates infarct size following coronary artery ligation-induced myocardial infarction (MI). C5ar1 deficiency limited the deposition of collagen and mitigated cell death in infarcted areas leading to overall improved cardiac function four weeks after MI. While infiltration of neutrophils was reduced in both C5ar1−/− and C5ar2−/− infarcted myocardium 24 h after MI, influx of monocytes after 1 week of MI was reduced only upon C5ar1 deficiency. Subsequent analysis revealed reduced accumulation of myofibroblast, elevated expression of transforming growth factor-beta1 (Tgf-β1) and vascular endothelial growth factor-A (Vegf-A) in C5ar1−/− infarcted hearts. In vitro, exogenous TGF-β1 triggered conversion of fibroblasts into myofibroblasts, which expressed Vegf-A mRNA – an effect that was enhanced upon C5ar1 deficiency. Incubation of C5ar1+/+ or C5ar1−/− endothelial cells (ECs) with supernatants from C5ar1+/+ or C5ar1−/− myofibroblasts respectively, mimicking the in vivo microenvironment in our model, led to significant increase in matrigel tube formation in C5ar1−/− ECs. This was consistent with enhanced neoangiogenesis in C5ar1−/− infarcted hearts. Collectively, our study demonstrates that inhibition of C5aR1 has the potential to improve cardiac function after myocardial infarction.

Corresponding Author:
Dr. Erdenechimeg Shagdarsuren, Heinrich-Heine-Universitat Dusseldorf Medizinische Fakultat, Dusseldorf, Germany, Erdenechimeg.Guenther@med.uni-duesseldorf.de

Affiliations:
Yaw Asare, Klinikum der Ludwig-Maximilians-Universität München, Institute for Stroke and Dementia Research (ISD), Munchen, Germany
Sakine Simsekyilmaz, RWTH Aachen University, Institute for Molecular Cardiovascular Research, RWTH Aachen University Hospital, Germany, Aachen, Germany
Janine Köhncke, RWTH Aachen University, Institute for Molecular Cardiovascular Research, RWTH Aachen University Hospital, Germany,

Aachen, Germany
[...]
Erdenechimeg Shagdarsuren, Heinrich-Heine-Universitat Dusseldorf Medizinische Fakultat, Dusseldorf, Germany

Cardiac repair after myocardial infarction is controlled by a complement C5a receptor 1-driven signaling cascade

Running title: Complement C5a receptors in cardiac repair

Yaw Asare, PhD[1]*, Sakine Simsekyilmaz, PhD[2]; Janine Köhncke, PhD[2]; Gansuvd Shagdarsuren, PhD[3], Mareike Staudt, MSc[2], Heidi Noels, PhD[2], Andreas Klos, MD[4], Johannes C. Fischer, MD[5], Jürgen Bernhagen, PhD[1,6], Alma Zernecke, MD[7], Elisa A. Liehn, MD, PhD[8,9,10], Erdenechimeg Shagdarsuren, MD[5]*

[1]Institute for Stroke and Dementia Research, University Hospital, Ludwig Maximilian University, Germany; [2]Institute for Molecular Cardiovascular Research, RWTH Aachen University Hospital, Germany; [3]Department of Nephrology, School of Medicine, Mongolian National University of Medical Sciences, Ulaanbaatar, Mongolia; [4]Department for Medical Microbiology, Hannover Medical School, Germany; [5]Institute for Transplantation Diagnostics and Cell Therapeutics, University Hospital and Medical Faculty, Heinrich Heine University Düsseldorf, Germany; [6]German Center for Cardiovascular Research (DZHK), Partner Site Munich Heart Alliance (MHA), Munich, Germany; [7]Institute of Experimental Biomedicine, University Hospital Würzburg, Germany; [8]Institute for Molecular Medicine, University of Southern Denmark, Odense, Denmark; [9]National Heart Center Singapore; [10]"Victor Babes" National Institute for Pathology, Bucharest, Romania

*Correspondence:

Erdenechimeg Shagdarsuren, MD
Institute for Transplantation Diagnostics and Cell Therapeutics, University Hospital and Medical Faculty, Heinrich Heine University Düsseldorf, Germany
Email: Erdenechimeg.Guenther@med.uni-duesseldorf.de

Yaw Asare, PhD
Institute for Stroke and Dementia Research, University Hospital, Ludwig-Maximilian University, Germany
E-mail: yaw.asare@med.uni-muenchen.de

Key words: cardiac repair, myocardial infarction, complement C5a receptors, and neoangiogenesis.

Heart Failure (HF) is a chronic medical condition characterized by the heart's inability to efficiently pump blood, often resulting from recurrent myocardial infarctions (1, 2). Despite improvements in risk management and interventional strategies, HF presents significant healthcare challenges and leads to increased healthcare expenditure due to gaps in HF therapy targets (3). Therefore, it is essential to identify treatable traits (4). Cardiac repair is a highly regulated process consisting of inflammatory, proliferation, and remodeling phases overlapping each other. This follows necrotic loss of cardiomyocytes after myocardial infarction (MI) in an attempt to repair the damage and restore heart function. Mechanisms in the repair process following MI include activation of the complement system as part of the innate immune response. The complement anaphylatoxin C5a interacts primarily with its two receptors, the classical pro-inflammatory C5a receptor 1 (C5aR1, CD88) and C5a receptor 2 (C5aR2, C5L2 (C5a receptor like 2)). Previous studies have implicated C5aR1 in cardiac regeneration after left ventricular apical resection (5) and cardiac inflammation (6, 7).

However, its role in cardiac repair processes following MI is poorly defined and the role of C5aR2 in MI is largely unknown. Our current study focused on late phases after MI up to 4 weeks after the infarction insult, a time window that specifically reflects the outcome of the repair process and that so far has not been investigated. Using *C5ar1*- and *C5ar2*-deficient mice, we studied the role of both C5aR1 and C5aR2 in cardiac function and repair processes following MI. We combined functional analyses and mechanistic studies *in vivo* and *in vitro* to demonstrate that targeting C5aR1 may provide a potent lever to improve cardiac repair after MI.

To systematically study the role of C5a receptors in cardiac repair processes following MI, wild-type C57Bl/6J, *C5ar1*$^{-/-}$ and *C5ar2*$^{-/-}$ mice were investigated after chronically ligating the left anterior descending artery (LAD). Histological analysis revealed a significantly reduced MI size **(Fig. 1a, b)** as well as lower collagen content in the infarcted area **(Fig. 1c and Supplementary Fig. 1a)** in *C5ar1*$^{-/-}$ mice compared to wildtype mice 4 weeks after MI. Infarct size and collagen content were not reduced in *C5ar2*$^{-/-}$ mice. This indicated a protective effect of *C5ar1* deficiency in MI. Consistent with the reduced MI size, *C5ar1*$^{-/-}$ mice showed a significantly increased ejection fraction and reduced end-diastolic volume when compared to wildtype mice 4 weeks after MI, indicating an improved ventricular function and contractility (**Supplementary Table 1**). Cardiac repair after MI relies on an intense inflammatory response that provides molecular cues for activation of reparative cells (8). As recruitment of inflammatory cells and the proliferation of tissue-resident macrophages in later stages are pivotal in this process, we analyzed the content of monocytes/macrophages and neutrophils in the infarcted areas. One week after induction of MI, the content of Mac3-positive monocytes/macrophages in the infarcted area peaked in wildtype mice and was significantly reduced in *C5ar1*$^{-/-}$ mice by 43% (**Fig. 1d, e and Supplementary Fig. 1b**). This peak of monocyte/macrophage accumulation drastically lowered at 4 weeks after MI without significant differences between groups (**Fig. 1e**). In contrast, the content of MPO+ cardiac neutrophils transiently increased 24 h after MI in wildtype mice and this increase was significantly reduced in both *C5ar1*$^{-/-}$ and *C5ar2*$^{-/-}$ mice (**Supplementary Fig. 2**). The reduced neutrophil accumulation in the infarcted heart could provide some cardioprotective effects in both *C5ar1*$^{-/-}$ and *C5ar2*$^{-/-}$ mice. However, the observation that infarction size was only reduced in *C5ar1*$^{-/-}$ mice suggested a predominant involvement of another C5ar1-mediated mechanism in cardiac repair after MI, urging us to also examine effects on cell proliferation vs. apoptosis and the expression of genes implicated in the late phase of cardiac repair. At one week, cell proliferation in the infarcted heart increased and the number of proliferating cells was significantly further increased in both *C5ar1*$^{-/-}$ and *C5ar2*$^{-/-}$ mice compared to control wildtype mice **(Supplementary Fig. 3a, b)**. Myocardial necrosis resulting from improper blood perfusion to the cardiac tissue after MI is a detrimental event, and cardiac repair mechanisms aim at removing necrotic tissue while inducing neovascularization. We therefore also examined the effect of *C5ar1* deficiency on myocardial necrosis *in vivo* and found reduced necrosis in *C5ar1*-deficient hearts 24 h after MI (**Supplementary Fig. 3c-e**). Likewise, *C5ar1* deficiency reduced apoptotic cells in the infarcted hearts (**Fig. 1f, g** and **Supplementary Fig. 3f, g**).

To further assess the mechanisms underlying the overall improved heart function upon *C5ar1* deficiency, we determined gene expression of key repair cytokines in infarcted hearts from wildtype and *C5ar1*$^{-/-}$ mice that underwent MI. Four weeks after MI (complete healing and maturation of the scar), we found significantly increased expression of Tgf-β1 and Vegf-A both on protein and mRNA levels, in *C5ar1*$^{-/-}$ infarcted hearts, when compared to

corresponding control wildtype hearts, while the levels one week after MI were not significantly altered **(Fig. 1h-j and Supplementary Fig. 4a-d)**. We further observed an increased expression of *Vegf-A* in TGF-β1-stimulated cardiac fibroblasts (**Supplementary Fig. 4e).** TGF-β1 was described as having a transient role in macrophage polarization and myofibroblasts differentiation during healing after MI (9). Given the increased expression of Tgf-β1 and Vegf-A, a highly potent angiogenic agent, during the maturation of the scar, we reasoned that *C5ar1* deficiency may promote a transient myofibroblast differentiation response resulting in improved cardiac repair. Surprisingly though, while the number of cardiac myofibroblasts remained unchanged in both genotypes one week after MI (**Supplementary Fig. 4f, g**), the number of α-SMA$^+$ cells in the infarcted myocardium was significantly reduced in *C5ar1*$^{-/-}$ mice compared to wildtype controls 4 weeks after MI (**Fig. 1k, l**). To further scrutinize the effect of the increased expression of Tgf-β1 in *C5ar1*$^{-/-}$ mice, we isolated cardiac fibroblasts from wildtype mice and quantified the expression of C5ar1. We found considerable expression of C5ar1 in cardiac fibroblasts, which was not altered upon TGF-β1 stimulation (**Supplementary Fig. 5a-d**). We then asked whether C5a/C5aR1 signaling affects the TGF-β1-driven conversion of cardiac fibroblasts to myofibroblasts. Exposure of wildtype cardiac fibroblasts to TGF-β1 was able to induce transdifferentiation as determined by α-SMA expression, but this was independent of C5a/C5aR1 signaling (**Supplementary Fig. 5e**, **f**). As overall myofibroblast transdifferentiation was not affected upon *C5ar1* deficiency, we hypothesized that the regulatory response of these cells was skewed with consequences for myofibroblast function. To test this notion mechanistically, cardiac fibroblasts isolated from wildtype and *C5ar1*$^{-/-}$ mice were stimulated with TGF-β1. Analysis of mRNA and protein expression revealed a TGF-β1-induced upregulation of Vegf-A levels in wildtype myofibroblasts, which was significantly increased in *C5ar1*$^{-/-}$ myofibroblasts **(Fig. 1m and Supplementary Fig. 5g)**. This is an indication that C5aR1-deficient myofibroblasts may contribute to the VEGF pool in the myocardium, by increasing the balance towards a pro-angiogenic phenotype of cardiac fibroblasts. After MI, neovascularization in the border zone adjacent to the ischemic region helps to preserve cardiac function and attenuate adverse left ventricular-remodeling (10). Our observation that the expression of Vegf-A is significantly upregulated in *C5ar1*$^{-/-}$ myofibroblasts and in infarcted heart areas from *C5ar1*$^{-/-}$ mice, potentially in part through effects on intracellular signaling including ERK and p38 MAPKs (11), led us to reason that upon stimulation, cardiac myofibroblasts may be a source of Vegf-A for endothelial cells (ECs) to support neoangiogenesis. To investigate this, we performed matrigel tube formation assays, where wildtype-ECs were incubated with supernatants derived from stimulated wildtype-fibroblasts and *C5ar1*$^{-/-}$-ECs were exposed to *C5ar1*$^{-/-}$-myofibroblast supernatant, mimicking the *in vivo* microenvironment in our model. We found increased tube formation in *C5ar1*$^{-/-}$-ECs/*C5ar1*$^{-/-}$-myofibroblast co-cultures compared to cell responses elicited in wildtype-cells **(Fig. 1n, o)** indicating, to our knowledge, for the first time a C5a/C5aR1-axis-mediated EC-fibroblast interaction in neovessel formation during the cardiac repair process following MI. This was consistent with significantly improved neovascularization in infarcted heart areas from *C5ar1*$^{-/-}$ mice as revealed by increased newly formed CD31$^+$ blood vessels 4 weeks after MI **(Fig. 1p, q)**. Hence, the C5a/C5aR1-axis may mediate EC-fibroblast interactions in cardiac repair processes and contribute to improved heart function observed in *C5ar1*$^{-/-}$ mice 4 weeks after MI. The identified EC-fibroblast interaction requires additional studies to further scrutinize the role of C5ar1 in cardiac fibroblast activation and related mechanisms.

Collectively, the results presented here show that *C5ar1* deficiency i) reduces infarct size following MI and enhances overall cardiac function; ii) attenuates myocardial necrosis; and

iii) enhances VEGF production by myofibroblasts and EC-fibroblast interactions to promote neovascularization in the infarcted heart. Although the exact contribution of C5aR1 on ECs versus fibroblasts in this EC-fibroblast interaction remains to be further clarified, our findings overall demonstrate an important role for the C5a/C5aR1-axis in the late endogenous repair mechanism following MI. This could complement cardioprotective effects provided by *C5ar1* deficiency on other cell types including platelets, where *C5ar1* deficiency promotes tissue neovascularization by reducing C5a-triggered secretion of the anti-angiogenic factor CXCL4 (12). Also, other immune cells including dendritic cells and $CD4^+$ T cells have been implicated in left ventricular remodeling and the progression of cardiac dysfunction following MI (13, 14) . As C5aR1 has been shown to regulate the function of both dendritic cells and $CD4^+$ T cells (15, 16), we cannot exclude effects of C5aR1 on these cells in the current study. Considering the pleiotropic role of C5aR1 in various cell types and signaling pathways, it is crucial to dissect in future studies the precise cell-specific C5aR1-dependent mechanisms involved in all phases of healing after MI: the acute inflammatory phase, the intermediate proliferation phase, and the late fibrosis phase. Unveiling the distinct, cell type- and time-dependent functions of C5aR1 signaling could further support the design of personalized therapeutic strategies to improve cardiac repair after MI.

Data availability

All data and materials are presented in the main manuscript or supplementary materials and are available on reasonable request.

References

1. Roger VL. Epidemiology of Heart Failure: A Contemporary Perspective. Circ Res. 2021;128(10):1421-34.

2. Dunlay SM, Roger VL, Redfield MM. Epidemiology of heart failure with preserved ejection fraction. Nat Rev Cardiol. 2017;14(10):591-602.

3. Savarese G, Becher PM, Lund LH, Seferovic P, Rosano GMC, Coats AJS. Global burden of heart failure: a comprehensive and updated review of epidemiology. Cardiovasc Res. 2023;118(17):3272-87.

4. Maslove DM, Tang B, Shankar-Hari M, Lawler PR, Angus DC, Baillie JK, et al. Redefining critical illness. Nat Med. 2022;28(6):1141-8.

5. Natarajan N, Abbas Y, Bryant DM, Gonzalez-Rosa JM, Sharpe M, Uygur A, et al. Complement Receptor C5aR1 Plays an Evolutionarily Conserved Role in Successful Cardiac Regeneration. Circulation. 2018;137(20):2152-65.

6. De Hoog VC, Timmers L, Van Duijvenvoorde A, De Jager SC, Van Middelaar BJ, Smeets MB, et al. Leucocyte expression of complement C5a receptors exacerbates infarct size after myocardial reperfusion injury. Cardiovasc Res. 2014;103(4):521-9.

7. Zhang C, Li Y, Wang C, Wu Y, Cui W, Miwa T, et al. Complement 5a receptor mediates angiotensin II-induced cardiac inflammation and remodeling. Arterioscler Thromb Vasc Biol. 2014;34(6):1240-8.

8. Frangogiannis NG. The inflammatory response in myocardial injury, repair, and remodelling. Nat Rev Cardiol. 2014;11(5):255-65.

9. Horckmans M, Ring L, Duchene J, Santovito D, Schloss MJ, Drechsler M, et al. Neutrophils orchestrate post-myocardial infarction healing by polarizing macrophages towards a reparative phenotype. Eur Heart J. 2017;38(3):187-97.

10. Liehn EA, Tuchscheerer N, Kanzler I, Drechsler M, Fraemohs L, Schuh A, et al. Double-edged role of the CXCL12/CXCR4 axis in experimental myocardial infarction. J Am Coll Cardiol. 2011;58(23):2415-23.

11. Nabizadeh JA, Manthey HD, Panagides N, Steyn FJ, Lee JD, Li XX, et al. C5a receptors C5aR1 and C5aR2 mediate opposing pathologies in a mouse model of melanoma. FASEB J. 2019;33(10):11060-71.

12. Nording H, Baron L, Haberthur D, Emschermann F, Mezger M, Sauter M, et al. The C5a/C5a receptor 1 axis controls tissue neovascularization through CXCL4 release from platelets. Nat Commun. 2021;12(1):3352.

13. Forte E, Perkins B, Sintou A, Kalkat HS, Papanikolaou A, Jenkins C, et al. Cross-Priming Dendritic Cells Exacerbate Immunopathology After Ischemic Tissue Damage in the Heart. Circulation. 2021;143(8):821-36.

14. Kumar V, Prabhu SD, Bansal SS. CD4(+) T-lymphocytes exhibit biphasic kinetics post-myocardial infarction. Front Cardiovasc Med. 2022;9:992653.

15. Verghese DA, Chun N, Paz K, Fribourg M, Woodruff TM, Flynn R, et al. C5aR1 regulates T follicular helper differentiation and chronic graft-versus-host disease bronchiolitis obliterans. JCI Insight. 2018;3(24).

16. Nguyen H, Kuril S, Bastian D, Kim J, Zhang M, Vaena SG, et al. Complement C3a and C5a receptors promote GVHD by suppressing mitophagy in recipient dendritic cells. JCI Insight. 2018;3(24).

Acknowledgements
We thank Roya Soltan, Yuan Kong, Tanja Vajen, Adelina Curaj, Melanie Garbe, and Stefanie Elbin for excellent technical assistance. This work was supported by Deutsche Forschungsgemeinschaft (DFG; CRC 1123 [B3]; and AS 575/1-1) grant to Y. Asare. J. Bernhagen acknowledges support from DFG (CRC 1123 [A3] and LMUexc strategic partnerships with Singapore) as well as from the German Center for Cardiovascular Research (grant DZHK B 20-004 Extern/81X2600258). E. Shagdarsuren received funding from DFG (GU1223/3-1).

Contributions
Y.A. and E.S. designed research with input from E.L; Y.A., S.S., E.L., J.K., G.S., M.S., H.N. performed research, Y.A., E.S., E.L., S.S., A.K., A.Z., J.B. analyzed data; Y.A., and E.S. wrote the paper. All authors reviewed and edited the manuscript.

Ethics declarations

Competing interests
The authors declare no competing interests.

Ethics
All animal experiments were approved by local authorities (Landesamt für Natur, Umwelt und Verbraucherschutz Nordrhein-Westfalen, Germany) and complied with the German animal protection law (AZ: 8.87-50.10.35.09.088).

Fig 1. C5aR1 controls cardiac repair mechanisms following myocardial infarction. a-e, MI was induced by chronically ligating the left anterior descending artery (LAD). **a, b**) Histomorphometrical analysis of the infarcted myocardium 4 weeks after MI in WT, *C5ar1*$^{-/-}$ and *C5ar2*$^{-/-}$ mice (n=7-9 per group) as measured by planimetry. Shown are representative Gomori's 1-step trichrome-stained sections (**a**) and the quantification of infarcted areas (**b**). **c**, Quantification of collagen content in infarcted area. **d**) Representative immunostaining of MAC3+ monocytes/macrophages in infarcted myocardium analyzed 1 week after MI. **e**, Quantification of myocardial infiltration of Mac3+ monocytes/macrophages analyzed 1 day, 1 week and 4 weeks after MI. Cells were visualized by immunostaining and the quantification is presented as the percentage of positively stained cells of total cell count in infarcted area in field of view (FOV). n=4-6 per group. **f, g,** Apoptosis rate in infarcted myocardium 24 h after MI induction in WT and *C5ar1*$^{-/-}$ mice detected by TUNEL staining. Shown is representative immunostaining (f). The quantification of cells is presented as the percentage of positively stained cells per field of view infarcted area (g). A complete set of this data is presented in supplementary Fig. 3c, d. **h-j** MI was performed in WT and *C5ar1*$^{-/-}$ mice, thereafter, infarcted heart areas were isolated 4 weeks after infarction. Representative immunoblot (**h**) and corresponding quantification of Tgf-β1 **(i)** and Vegf-A **(j)** normalized to actin. Representative staining (**k**) and quantification (**l**) of SMA^{+}/CD31^{-}-myofibroblasts in the infarcted myocardium. White arrows indicate SMA^{+} myofibroblasts (green fluorescence). Scale bars 100 µm. **m**, Cardiac fibroblasts isolated from WT and *C5ar1*$^{-/-}$ mice were stimulated with TGF-β1 alone or together with C5a. Quantification of protein expression of Vegf-A normalized to actin. **n, o** Supernatant from TGF-β1-stimulated WT or *C5ar1*$^{-/-}$ cardiac fibroblasts were incubated on WT-ECs or *C5ar1*$^{-/-}$-ECs respectively, in a co-culture, and tube formation was determined in WT-ECs and *C5ar1*$^{-/-}$-ECs. Shown are representative images (n) and quantification of tube formation (o). **p, q,** Neoangiogenesis was assessed by CD31^{+}/α-SMA^{-}- staining of WT, and *C5ar1*$^{-/-}$ infarcted heart areas 4 weeks after infarction**. p,** Representative CD31 staining of infarcted heart areas and **q,** corresponding quantification. N = 7 mice per group. Data are presented as mean ± SEM.

Supplementary Materials

Cardiac repair after myocardial infarction is controlled by complement C5a receptor 1-driven signaling cascade

Running title: **Complement C5a receptors in cardiac repair**

Yaw Asare, PhD[1]*, Sakine Simsekyilmaz, PhD[2]; Janine Köhncke, PhD[2]; Gansuvd Shagdarsuren, PhD[3], Mareike Staudt, MSc[2], Heidi Noels, PhD[2], Andreas Klos, MD[4], Johannes C. Fischer, MD[5], Jürgen Bernhagen, PhD[1,6], Alma Zernecke, MD[7], Elisa A. Liehn, MD, PhD[8,9,10], Erdenechimeg Shagdarsuren, MD[5]*

[1]Institute for Stroke and Dementia Research, University Hospital, Ludwig Maximilian University, Germany; [2]Institute for Molecular Cardiovascular Research, RWTH Aachen University Hospital, Germany; [3]Department of Nephrology, School of Medicine, Mongolian National University of Medical Sciences, Ulaanbaatar, Mongolia; [4]Department for Medical Microbiology, Hannover Medical School, Germany; [5]Institute for Transplantation Diagnostics and Cell Therapeutics, University Hospital and Medical Faculty, Heinrich Heine University Düsseldorf, Germany; [6]German Center for Cardiovascular Research (DZHK), Partner Site Munich Heart Alliance (MHA), Munich, Germany; [7]Institute of Experimental Biomedicine, University Hospital Würzburg, Germany; [8]Institute for Molecular Medicine, University of Southern Denmark, Odense, Denmark; [9]National Heart Center Singapore; [10]"Victor Babes" National Institute for Pathology, Bucharest, Romania

*Correspondence:

Erdenechimeg Shagdarsuren, MD
Institute for Transplantation Diagnostics and Cell Therapeutics, University Hospital and Medical Faculty, Heinrich Heine University Düsseldorf, Germany
Email: Erdenechimeg.Guenther@med.uni-duesseldorf.de

Yaw Asare, PhD
Institute for Stroke and Dementia Research, University Hospital, Ludwig Maximilians University, Germany
E-mail: yaw.asare@med.uni-muenchen.de

Materials and Methods

Animal model of myocardial infarction

Wild-type C57Bl/6J (WT; Jackson Laboratory), *C5ar1*-deficient (*C5ar1*$^{-/-}$) or *C5ar2* -deficient mice (*C5ar2*$^{-/-}$) were kindly provided by Prof. A. Klos (Hannover Medical School, Germany). Female mice that were 12-weeks old and 6-8 per group were used in this study. Mice were intubated under general anesthesia and MI was performed as previously described(1). Briefly, after anesthetizing with Ketamine (100 mg/kg) and Xylazine (10 mg/kg) and treated with analgetic (Buprenorphine 100 µg/kg), MI was induced by chronically ligating the left anterior descending artery. The animals were treated with (Buprenorphine 100 µg/kg) for further 72 hours and were evaluated clinically daily. They were kept under standard conditions, with unlimited access to food and water for the next 24 hours, 1 week or 4 weeks after MI induction and then sacrificed. To avoid high mortality in mice and comply with the 3R principles, we have performed small size infarctions, which were sufficient to fulfil the purpose of this study. All animal experiments were approved by local authorities (Landesamt für Natur, Umwelt und Verbraucherschutz Nordrhein-Westfalen, Germany) and complied with the German animal protection law (AZ: 8.87-50.10.35.09.088, approved on 01.07.2010).

Echocardiography

Before and four weeks after MI, left ventricular (LV) function and LV volumes were determined by echocardiography performed on a small-animal ultrasound imager (Vevo 770, FUJIFILM Visual sonics). During the procedure, mice were sedated with 1.5% isoflurane. Female mice were used in all experiments. Measurements of the short and long parasternal axes were taken in B-Mode (2D-

realtime) and M-Mode using a 40-megahertz transducer. The left ventricular (LV) ejection fraction (EF) was assessed and analyzed in the long axis and in the short axis, obtained at the level of the papillary muscles. It is derived from the LV end-diastolic volume (LVEDV) and LV end-systolic volume (LVESV), which are calculated parameters from LV internal diameters (LVID systole and LVID diastole). The formula for calculating EF is EF % = (LVEDV-LVESV) / LVEDV x 100. Furthermore, we recorded and calculated cardiac output, heart rate (HR), LV weight and stroke volumes. SV = LVEDV – LVESV; Cardiac output (CO) = SV x HR (heart rate). All these followed the established standardized protocols for high-frequency ultrasound equipment (https://www.visualsonics.com/application/preclinical/cardiology) and as recommended by ESC Working Group on Myocardial Function (2).

Determination of MI size by histomorphometry and collagen quantification
Formalin-fixed, paraffin-embedded serial sections of the hearts were stained with Gomori's 1-step trichrome stain and the infarcted area and collagen content was quantified as previously described(1).

Immunofluorescence staining of inflammatory, proliferating and apoptotic cells, myofibroblasts and ECs
Serial sections, 3 per mouse and 200 µm apart, of mice that underwent MI for 24 h, 1 and 4 weeks were stained with primary antibodies for neutrophils (rabbit-anti-mouse MPO, Neomarkers), monocytes (rat-anti-mouse Mac-3, BD Pharmingen) and proliferating cells (anti-mouse Ki-67 antibody #M7249, clone TEC3, DakoCytomation). Apoptotic nuclei were detected by terminal deoxynucleotidyl dUTP nick-end labeling (TUNEL-kit, Roche), myofibroblasts by α-SMA (clone 1A4; Dako, Glostrup, Denmark) and ECs by rabbit-anti-PECAM (#M20, Santa Cruz, CA).

Evans-Blue/ Triphenyl tetrazolium chloride (TTC) staining
Area at risk (AAR) and infarct size were measured 24 h after MI. The hearts were excised (4 mice per group) and washed with PBS, the ligature over the LAD was renewed and 200 µl Evans-Blue was perfused through the aorta. After freezing at −20 °C for one hour, the hearts were cut in 5 slices, and incubated in tetrazolium solution (TTC) at 37 °C for 10 min, followed by 10% formaldehyde for 10 min. The slices were fixed between microscopic slides for photography and measurements. The total ventricle area, the blue-stained normally perfused area, red-stained injured but still viable area and white infarcted area were measured using ImageJ. AAR was calculated as the difference between the total and blue-stained area and expressed as percent of total ventricle area. Infarction size was calculated as white unstained area and expressed as percent of AAR.

Quantitative Real-Time PCR (qRT-PCR)
DNA-free total RNA was extracted from infarcted heart areas or cells using the Zymo RNA MiniPrep kit or MicroPrep kit (Zymo Research). RNA was reverse-transcribed using oligo-dT primers. qRT-PCR was performed using Express SybrGreenER qPCR Supermix (Invitrogen), specific primers and a thermal cycler (Applied Biosystems). β-actin or Gapdh was used as reference gene as indicated.

Isolation of fibroblasts and ECs
Cardiac fibroblasts were isolated from wildtype or *C5ar1*$^{-/-}$ mice by enzymatic digestion (Collagenase type I, Roche) as previously established (3, 4). Adherent fibroblasts were further cultured in Dulbecco ′s modified eagle′s medium: high glucose (DMEM, Sigma-Aldrich) containing 1% Penicillin/Streptomycin (Cölbe) and 10% serum (Fetal bovine serum dialyzed; PAN Biotech). As the other predominant cardiac cells including cardiomocytes, and ECs require specific growth factors and conditions for *in vitro* cultivation, they do not survive in the culture and are washed away. ECs from thoracic aorta of wildtype or *C5ar1*$^{-/-}$ mice were isolated using MACS CD105 MultiSort Kit (Miltenyi Biotech).

Western blot and flow cytometry
Western blot was carried out as previously described (5). Briefly, fibroblasts from WT mice were stimulated with TGF-β1 (New England Biolabs). Total cell lysates were separated by SDS-PAGE, transferred onto nitrocellulose membrane (Whatman), and detected with anti-C5aR1 (Santa Cruz Biotech S5/1) and anti-Actin (Abcam). Heart tissues from WT and *C5ar1*$^{-/-}$ mice were homogenized

und lysates were separated by SDS-PAGE, transferred onto nitrocellulose membrane (Whatman), and detected with anti-VEGF-A (Biolegend, Clone 1F07-2C01) and anti-TGF-β (MAB 73461, R&D systems). For flow cytometry, cells were stained with C5aR1 antibody (anti-mouse CD88-phycoerythrin rat IgG2a; Serotec) and analyzed in a FACSCanto II.

Myofibroblast transdifferentiation assay
Isolated cardiac fibroblasts were seeded on collagen-coated plates ($1x10^5$ cells per well) in appropriate medium and incubated with C5a (100 or 200 ng/ml) with or without TGF-ß1 (10 or 20 ng/ml) as indicated for 6h under normoxic conditions. Thereafter, cells were analyzed by qRT-PCR.

***In vitro* Matrigel tube formation assay**
Isolated ECs from wildtype or *C5ar1*$^{-/-}$ mice were used for tube formation assay. 100 µl of matrigel were placed and $1x10^4$ ECs in 100 µl in assay medium were seeded per well. After incubating the cells at 37°C for 16 h, tube formation ability was quantified. Furthermore, ECs from WT or *C5ar1*$^{-/-}$ mice were incubated with supernatant from C5a plus TGF-β-stimulated wildtype- or *C5ar1*$^{-/-}$ -fibroblasts, respectively, and analyzed for tube formation. The tube formation ability was quantified by counting the total number of tube-like structures in five randomly chosen microscopic fields.

Statistical analysis
All data are given as mean ± SEM and were analyzed for normality by Shapiro-Wilk test and then by two-tailed Student's *t* test, 1-way ANOVA followed by Newmann-Keuls, Holm-Sidak or Tukey's multiple comparison test, as appropriate, using Prism 9.0 software (GraphPad, CA). P-value < 0.05 was considered statistically significant.

References

1. Liehn EA, Merx MW, Postea O, Becher S, Djalali-Talab Y, Shagdarsuren E, et al. Ccr1 deficiency reduces inflammatory remodelling and preserves left ventricular function after myocardial infarction. J Cell Mol Med. 2008;12(2):496-506.
2. Zacchigna S, Paldino A, Falcao-Pires I, Daskalopoulos EP, Dal Ferro M, Vodret S, et al. Towards standardization of echocardiography for the evaluation of left ventricular function in adult rodents: a position paper of the ESC Working Group on Myocardial Function. Cardiovasc Res. 2021;117(1):43-59
3. Curaj A, Schumacher D, Rusu M, Staudt M, Li X, Simsekyilmaz S, et al. Neutrophils Modulate Fibroblast Function and Promote Healing and Scar Formation after Murine Myocardial Infarction. Int J Mol Sci. 2020;21(10).
4. Xu Y, Zheng H, Nilcham P, Bucur O, Vogt F, Slabu I, et al. Vitamin C Regulates the Profibrotic Activity of Fibroblasts in In Vitro Replica Settings of Myocardial Infarction. Int J Mol Sci. 2023;24(9).
5. Asare Y, Shagdarsuren E, Schmid JA, Tilstam PV, Grommes J, El Bounkari O, et al. Endothelial CSN5 impairs NF-kappaB activation and monocyte adhesion to endothelial cells and is highly expressed in human atherosclerotic lesions. Thromb Haemost. 2013;110(1):141-52.

Supplementary TABLE 1 Cardiac function parameters before and 4 weeks after MI

Cardiac function parameters		
	Pre-MI	**4 weeks after MI**

	WT	***C5ar1*$^{-/-}$**	***C5ar2*$^{-/-}$**	***WT***	***C5ar1*$^{-/-}$**	***C5ar2*$^{-/-}$**
Heart rate (bpm)	340.5± 20.9	409.9± 62.5	476.1± 42.5 †	395.3± 35.7	561.8± 39.2** ‡	565.0± 51.7* ‡
Cardiac output (mL/min)	18.4 ± 1.7	19.5 ± 2.2	18.4 ±1.3	19.6 ± 2.3	19.6 ± 1.4	19.2 ± 1.2
Volume, d (µL)	55.5 ± 3.6	59.8± 1.9	48.6 ± 3.2	80.3 ± 4.3‡	65.0 ± 4.4*	70.2 ± 5.0‡
Volume, s (µL)	29.5 ± 2.2	36.7 ± 2.6	23.2 ± 2.5	41.7 ± 2.3‡	37.7 ± 3.8	44.6 ± 3.3‡
Stroke volume, s (µL)	25.9 ± 1.6	23.6 ± 0.6	24.9 ± 1.2	37.0 ± 1.7‡	26.0 ± 1.3*	25.5 ± 1.0
Ejection fraction (%)	51.7 ± 1.5	52.5 ± 1.6	52.9 ± 2.5	41.6 ± 1.9‡	49.6 ± 1.4*	42.1 ± 1.4 ‡
LV weight (mg)	84.6 ± 5.3	79.4 ± 7.6	81.0 ± 5.0	157.5 ±10.2‡‡	99.2 ± 6.9** ‡	117.7 ± 8.9* ‡

MI – myocardial infarction, LV – Left Ventricular, bmp – beats per minute, d – diastolic, s – systolic

* p<0.05, ** p<0.005, *WT*-control vs. *C5ar1*$^{-/-}$ *or C5ar2*$^{-/-}$ after MI,

† p<0.05, *WT*-control vs. *C5ar1*$^{-/-}$ *or C5ar2*$^{-/-}$ before MI,

‡ p<0.05, ‡‡ p<0.005, before MI vs. after MI, *WT*-control, *C5ar1*$^{-/-}$ and *C5ar2*$^{-/-}$

Supplementary Figures

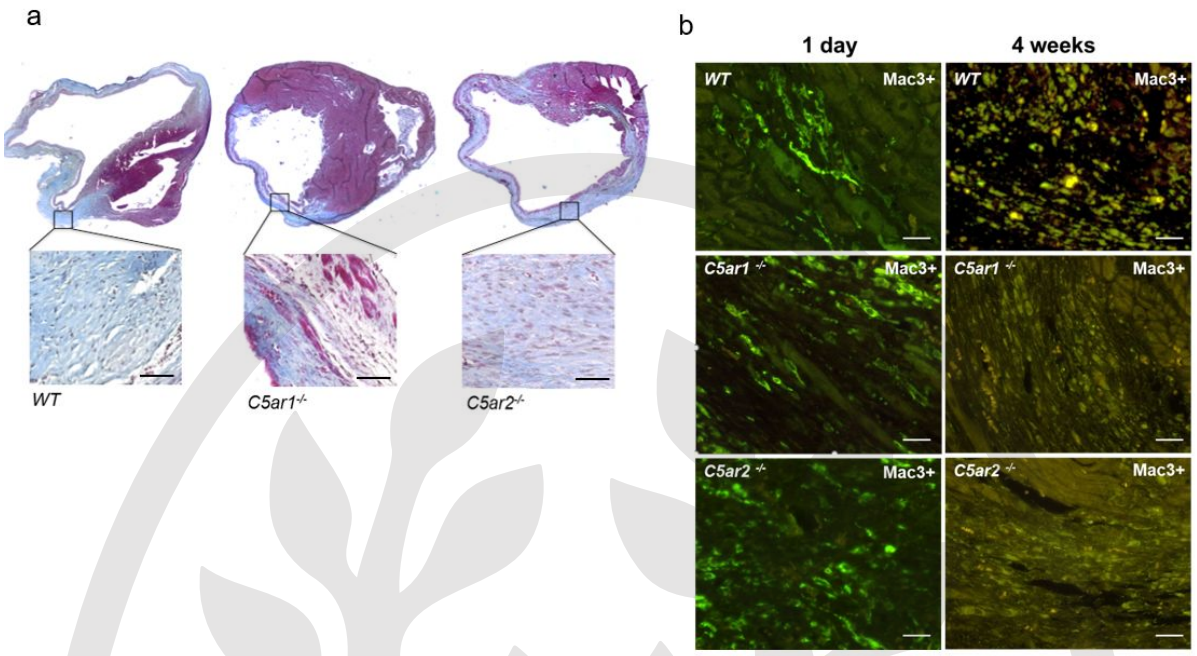

Figure S1. Collagen content and macrophage accumulation in the infarcted areas. a, Representative collagen stainings. Scale bars 50 µm. The quantification is shown in Fig. 1b. b, Representative images of myocardial infiltration of Mac3+ monocytes/macrophages into the infarcted myocardium assessed 1 day and 4 weeks after MI. The quantification is shown in Fig. 1f. Cells were visualized by MAC3 immunostaining (green fluorescence). Scale bars 50 µm.

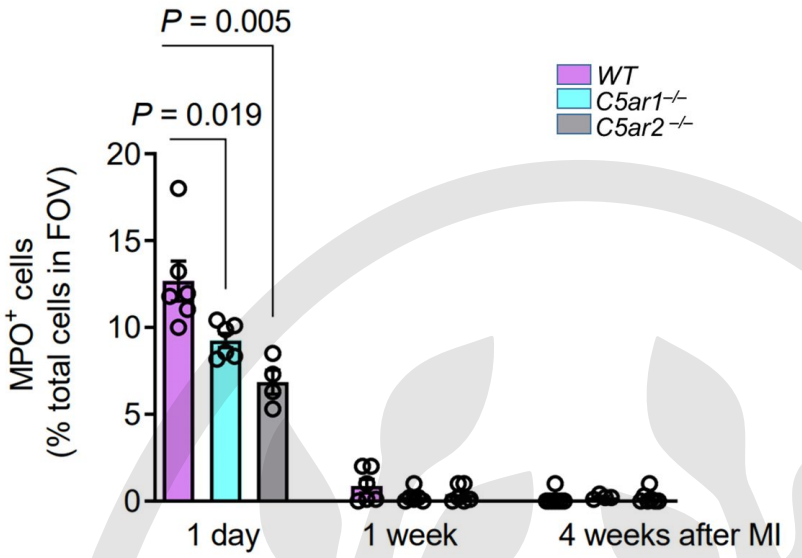

Figure S2. Analysis of neutrophil infiltration into infarcted areas.

Quantification of myocardial infiltration of MPO+ cells into the infarcted myocardium analyzed 1 day, 1 week and 4 weeks after MI. Cells were visualized by MPO immunostaining and quantified as percent of total DAPI+ cells in field of view. Data are presented as mean ± SEM. Each data point represents an independent mouse.

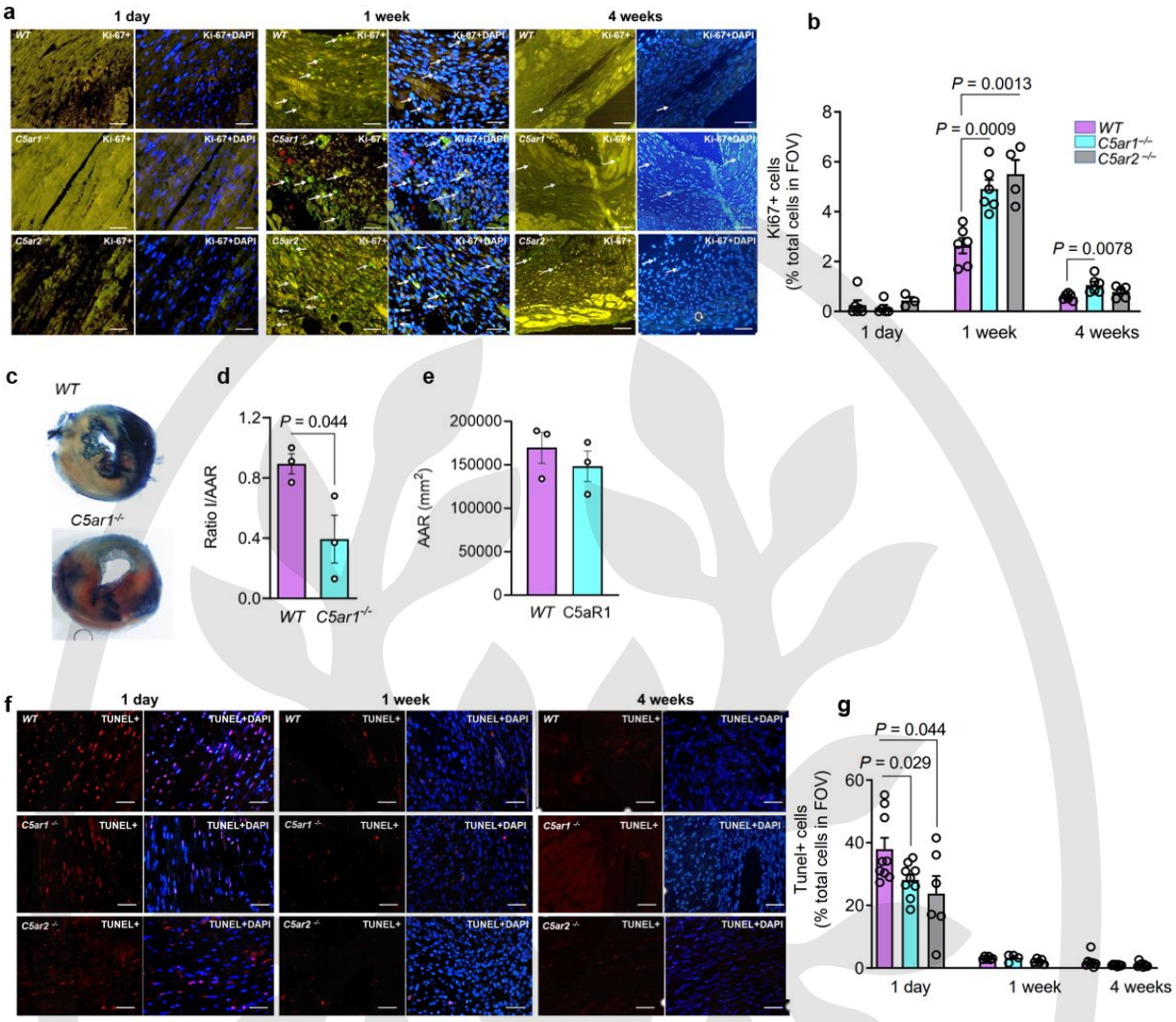

Figure S3. Proliferation and apoptosis rate in *C5ar1*- and *C5ar2*-deficient mice after MI.

a, b) Proliferation rate in infarcted myocardium 1 day, 1 or 4 weeks after MI-induction in WT, *C5ar1*$^{-/-}$ and *C5ar2*$^{-/-}$ mice detected by immunohistochemical staining of Ki-67+ cells. Representative immunostaining, green fluorescence for Ki-67+ cells, merged images with DAPI are shown. Arrows indicate positively stained cells. Scale bars 50 μm (**a**), and quantification (**b**) of Ki-67+ cells. n = 4-6 mice. **c-e**, MI was performed in *WT* and *C5ar1*$^{-/-}$ mice and infarcted hearts were isolated 24 h after infarction for analysis of the infarcted area and the area at risk (AAR) using a combination of Evans-blue injection and TTC staining. **c**, Representative TTC-stained hearts and **d**, corresponding quantification depicted as white unstained area and expressed as percent of AAR (area at risk; I/AAR (infarction size/ area at risk). **e**, absolute AAR. **f, g**) Apoptosis rate in infarcted myocardium 1 day, 1 or 4 weeks after MI induction in WT, *C5ar1*$^{-/-}$ and *C5ar2*$^{-/-}$ mice detected by TUNEL staining. Representative immunostaining, red fluorescence for TUNEL+ cells, merged image with DAPI are shown. Scale bars 50 μm. Shown is representative immunostaining (**f**). The quantification of cells in **(g)** is presented as the percentage of positively stained cells field of view infarcted area. Data are presented as mean ± SEM. Each data point represents an independent mouse.

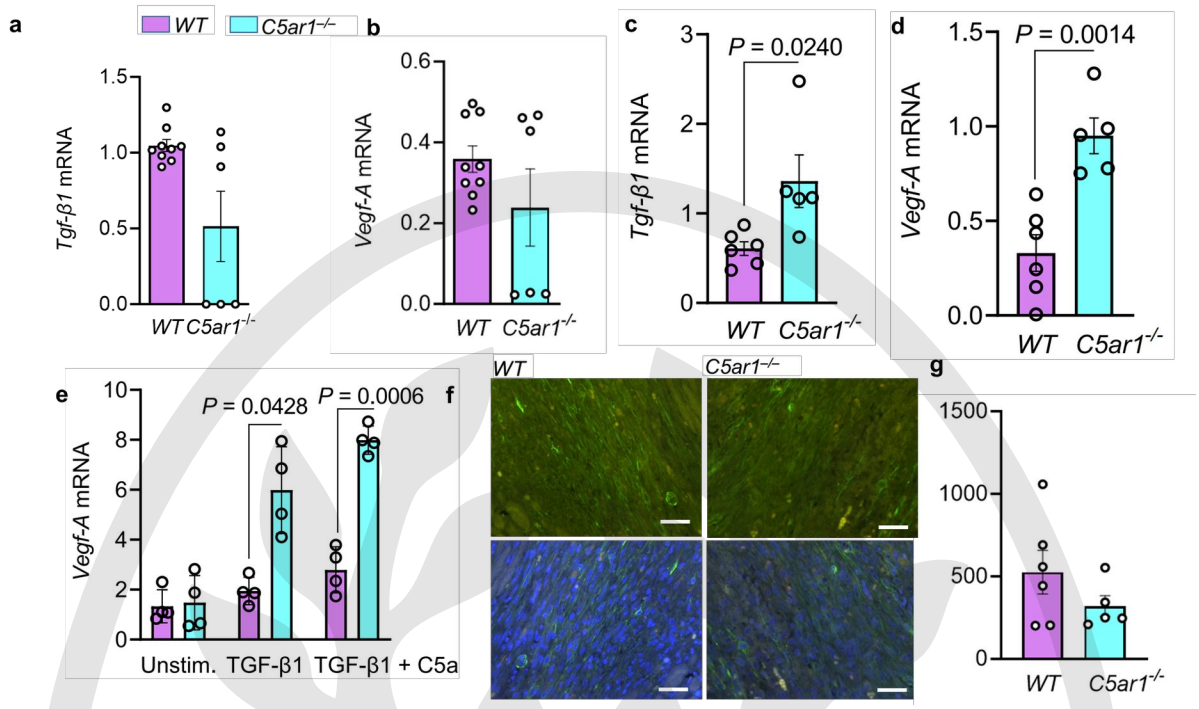

Figure S4. Cytokine analysis of infarcted heart areas and cardiac fibroblasts/myofibroblasts.

a, **b)** MI was performed in *WT* and *C5ar1*$^{-/-}$ mice, thereafter, infarcted heart areas were isolated either 1 week (a, b) or 4 weeks (c, d) after surgery. Quantification of *Tgf-β1* (**a**) and *Vegf-A* (**b**) gene expression normalized to Gapdh 1 week after MI. Quantification of *Tgf-β1* (**c**) and *Vegf-A* (**d**) gene expression normalized to Gapdh 4 weeks after MI. **e)** Analysis of *Vegf-A* mRNA levels in cardiac fibroblasts following TGF-β1 stimulation with or without C5a-exposure. **F,g**) Representative α-SMA positive staining **f**), quantification of SMA^{+} myofibroblasts in the infarcted myocardium 1 week after MI. Data are presented as mean ± SEM. Each data point represents an independent mouse.

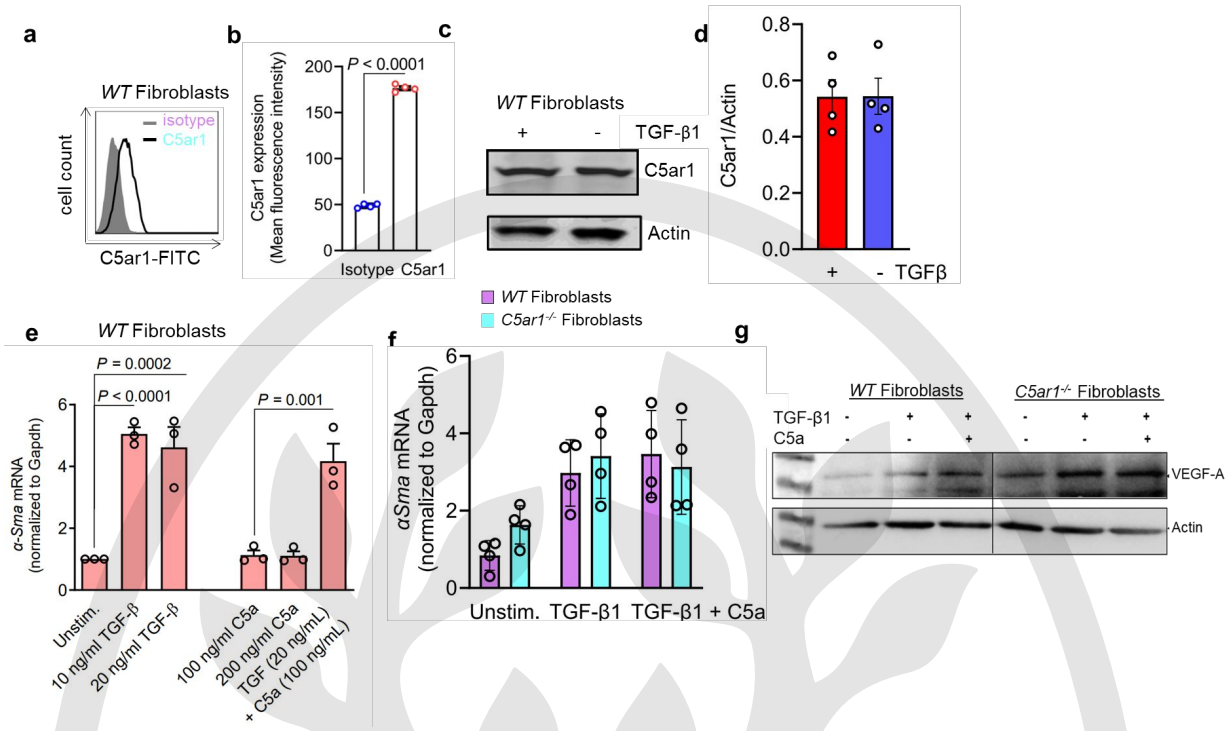

Figure S5. Analysis of cardiac fibroblasts/myofibroblasts *in vitro*. Quantification of C5ar1-expressing primary cardiac WT-fibroblasts by flow cytometry **(a, b)** and immunoblotting (**c, d**). **e,f)** Quantification of α-SMA mRNA expression, indicative of fibroblast-to-myofibroblast transdifferentiation, upon TGF-β1 stimulation with or without C5a exposure. **g,** Analysis of Vegf-A levels in cardiac fibroblasts following TGF-β1 stimulation with or without C5a-exposure. Shown is a representative immunoblot as quantified in Fig. 1. Each data point represents an independent isolation.

What is known about this topic?

Cardiac repair is a highly regulated process consisting of inflammatory, proliferation, and remodeling phases overlapping each other.

C5aR1 is implicated in cardiac regeneration after left ventricular apical resection and cardiac inflammation.

What does this paper add?

We show that *C5ar1* deficiency reduces infarct size following MI, attenuates myocardial necrosis, and enhances overall cardiac function.

We demonstrate that C5aR1 regulates EC-fibroblast interactions to promote neovascularization in the infarcted heart.